

**On the impacts of roadway hierarchical on the network Macroscopic
Fundamental Diagram**

By

Guanhao Xu

Department of Civil and Environmental Engineering
The Pennsylvania State University
201 Transportation Research Building
University Park, PA 16802
Phone: 217-974-0536
gux13@psu.edu

Vikash V. Gayah*

Department of Civil and Environmental Engineering
The Pennsylvania State University
231L Sackett Building
University Park, PA 16802
Phone: 814-865-4014
gayah@engr.psu.edu

***Corresponding Author**

July 2020

Word count: 7,155 (6,655 + 2 tables)

1 ABSTRACT

2 Relationships between average network productivity and accumulation or density aggregated
3 across spatially compact regions of urban networks—so called network Macroscopic Fundamental
4 Diagrams (MFDs)—have recently been shown to exist. Various analytical methods have been put
5 forward to estimate a network's MFD as a function of network properties, such as average block
6 lengths, signal timings and traffic flow characteristics on links. However, real street networks are
7 not homogeneous—they generally have a hierarchical structure where some streets (e.g., arterials)
8 promote higher mobility than others (e.g., local roads). This paper provides an analytical method
9 to estimate the MFDs of hierarchical street networks by considering features that are specific to
10 hierarchical network structures. Since the performance of hierarchical networks is driven by how
11 vehicles are routed across the different street types, two routing conditions—user equilibrium and
12 system optimal routing—are considered in the analytical model. The proposed method is first
13 implemented to describe the MFD of a hierarchical one-way limited access linear corridor and
14 then extended to a more realistic hierarchical two-dimensional grid network. For both cases, it is
15 shown that the MFD of a hierarchical network may no longer be unimodal or concave as
16 traditionally assumed in most MFD-based modeling frameworks. These findings are verified using
17 simulations of hierarchical corridors. Finally, the proposed methodology is applied to demonstrate
18 how it can be used to make decisions related to the design of hierarchical street network structures.
19

1 INTRODUCTION

2 Although aggregate (network-wide) traffic relationships have been studied intermittently for
3 nearly 50 years (1–3), empirical confirmation of well-defined relationships just over a decade ago
4 (4) has led to a renewed interest in this topic. This most recent study showed that a unimodal
5 relationship exists between the average productivity and accumulation/density of vehicles
6 traveling on a network using data from Yokohama, Japan. Such relationships are commonly
7 referred to as network Macroscopic Fundamental Diagrams or MFDs. When present, MFDs can
8 be used to model traffic dynamics within an urban network by dividing the network into a set of
9 spatially compact homogeneous regions and tracking the average level of congestion in each (5).
10 A variety of regional traffic control studies have been developed using this MFD-based
11 representation of urban traffic networks; recent relevant examples in the literature include
12 perimeter metering control (6–8), pricing (9, 10) and street network design (11, 12). Additional
13 studies have examined situations or properties that are necessary for well-defined MFDs to exist
14 (13–17).

15 Various studies have proposed methods to estimate a network's MFD using different data
16 sources (18–21). However, very few empirical derived MFDs exist in the literature, due to a lack
17 of data availability to quantify existing relationships on real networks (22–27). Thus, analytical
18 methods have been proposed to estimate a network's MFD as a function of various network
19 properties, such as average block lengths, signal timings and traffic flow characteristics on links
20 (28–32). These methods abstract a network into a single, infinitely long corridor and apply the
21 variational theory of kinematic waves (33–35) to estimate the average flow-density relationship
22 along the corridor. These existing methods can be applied to networks made up of homogeneous
23 networks made up of similar link types. However, real street networks are far from
24 homogeneous—they generally tend to have a hierarchical structure where some streets (e.g.,
25 arterials) promote higher mobility than others (e.g., local roads).

26 Very few studies have considered the impacts of street network hierarchy on MFDs. One
27 related study used simulation to examine how MFDs might change when links were removed in a
28 grid network, which might create unintentional hierarchies (36). Knoop et al. (37) examined how
29 various combinations of arterial and local street network patterns may influence the shape of the
30 MFD using simulation. Network structures were generated randomly so they could not be directly
31 compared. Muhlich et al. (38) used simulation to study flow-density relationships during
32 congestion onset and dissipation when arterial streets were mixed with local streets. However,
33 these previous studies all relied on simulation and thus they could not be used to determine general
34 features that might arise in MFDs of hierarchical network structures.

35 In light of this, this paper studies the MFDs of hierarchical street networks analytically to
36 unveil features that should be generally expected in real-world MFDs. This work directly builds
37 on a recent study that considers the MFDs of simple networks with route choice (30) by
38 considering features that are specific to hierarchical network structures. The results contribute to
39 the growing literature on relationships between traffic variables aggregated across large spatial
40 regions and how these relationships are influenced by network features.

41 The remainder of this paper is organized as follows. First, methods to estimate the MFD of
42 a hierarchical linear corridor are described. This includes verification of the proposed methods
43 within a simulation environment and application of this model to inform street network design.

1 Then, the methods are extended to hierarchical, two-dimensional grid networks. Finally, some
 2 discussion of these methods and results are provided.

3

4 **HIERARCHICAL ONE-WAY LINEAR CORRIDOR WITH LIMITED ACCESS**

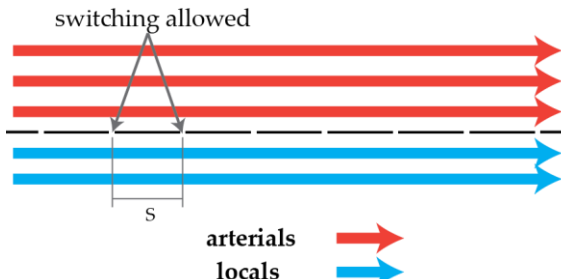
5 We first consider a one-way linear corridor system. Without loss of generality, we assume two
 6 street types are available: arterials (a) and local roads (l). A well-defined MFD is assumed to exist
 7 for each roadway type $i \in \{a, l\}$ that relates its average flow, q_i , to its average density, k_i . We
 8 denote this MFD $Q_i(k)$, where $q_i = Q_i(k_i)$. Note also that the average travel speed on each
 9 roadway type i is a function of the density on that roadway type and the MFD, $v_i = V_i(k_i) =$
 10 $Q_i(k_i)/k_i$. If the total length of each roadway type, L_i [lane-mile], is also known, the average flow
 11 (q_T) and density (k_t) on the entire corridor system can be determined using the generalized
 12 definitions of Edie (39) and written as:

13
$$q_H = \frac{q_a L_a + q_l L_l}{L_a + L_l} \quad (1.1)$$

14
$$k_H = \frac{k_a L_a + k_l L_l}{L_a + L_l} \quad (1.2)$$

15 We assume that vehicles cannot switch freely between the two roadway types. Instead,
 16 vehicles can only travel between the two roadway types at predesignated points located some
 17 distance S [mile] apart; see FIGURE 1. These switching locations are analogous to intersections
 18 in a two-dimensional network where vehicles can turn from one roadway type to another. In a
 19 linear corridor, this would represent access points. Such access points exist in several linear
 20 transportation facilities; e.g., HOV lanes with limited entry locations.

21



22
 23 **FIGURE 1. Graphical depiction of linear corridor.**

24

25 We also assume that p_l percent of trips begin and end on local roads and that p_a percent of
 26 trips begin and end arterials ($p_l + p_a = 1$). Therefore, there are four types of origin-destination
 27 (OD) pairs: both origin and destination on local (LL), origin on local and destination on arterial
 28 (LA), origin on arterial and destination on local (AL), and both origin and destination on arterial
 29 (AA).

30

1 **Analytical method to obtain the system-wide MFD**

2 This section describes how the average flow-density relationship of the combined corridor (i.e.,
 3 the MFD of the hierarchical linear network) can be estimated. We assume that each vehicle has
 4 two routing options to complete its trip: 1) primarily use local roads (i.e., only use arterials to
 5 access the local roads); or, 2) primarily use arterials (i.e., only use local roads to access the
 6 arterials). For example, consider the LL OD case. Under strategy 1, vehicles will stay on the local
 7 roads for their entire trip, while under strategy 2 vehicles will use the local roads to access the
 8 arterial, travel on the arterial to approach their destination, and then use local roads to access their
 9 destination.

10 Let D be the average shortest-path distance between OD pairs. If the spatial distributions
 11 of origins and destinations are known, then the average distance traveled per trip on roadway type
 12 i under each combination of routing option j ($j = 1$ or 2) and OD pair z ($z = LL, LA, AL$, or AA),
 13 $D_i^j(z)$, can be estimated using continuum approximation principles, as in (40). TABLE 1 provides
 14 these values for all OD pair-routing option combinations and the percentage of each type of OD
 15 pair, $P(z)$, assuming that origins and destinations on each roadway type are distributed uniformly
 16 in space.

17
 18 TABLE 1. Average trip distance on each roadway type

OD pair z	Percentage of OD pairs, $P(z)$	Strategy 1		Strategy 2	
		$D_l^1(z)$	$D_a^1(z)$	$D_l^2(z)$	$D_a^2(z)$
LL	p_l^2	D	0	S	$D - S$
LA	$p_l \cdot p_a$	$D - \frac{S}{2}$	$\frac{S}{2}$	$\frac{S}{2}$	$D - \frac{S}{2}$
AL	$p_l \cdot p_a$	$D - \frac{S}{2}$	$\frac{S}{2}$	$\frac{S}{2}$	$D - \frac{S}{2}$
AA	p_a^2	$D - S$	S	0	D

19
 20 Denote the fraction of vehicles that use strategy 1 are p . The ratio of flow on the arterial
 21 and local roads would be related by the total distance traveled on each of the two roadway types
 22 as per the generalized definitions of flow (39) as follows:

$$\begin{aligned}
 23 \quad \frac{q_l}{q_a} &= \frac{L_a}{L_l} \times \frac{[p \times \sum_z P(z) \times D_l^1(z) + (1-p) \times \sum_z P(z) \times D_l^2(z)]}{[p \times \sum_z P(z) \times D_a^1(z) + (1-p) \times \sum_z P(z) \times D_a^2(z)]} \\
 24 \quad &= \frac{L_a}{L_l} \times \frac{p \times [p_l^2 \times D + 2 \times p_l p_a \times (D - \frac{S}{2}) + p_a^2 \times (D - S)] + (1-p) \times [p_l^2 \times S + 2 \times p_l p_a \times \frac{S}{2} + p_a^2 \times 0]}{p \times [p_l^2 \times 0 + 2 \times p_l p_a \times \frac{S}{2} + p_a^2 \times S] + (1-p) \times [p_l^2 \times (D - S) + 2 \times p_l p_a \times (D - \frac{S}{2}) + p_a^2 \times D]} \quad (2)
 \end{aligned}$$

25 For given values of p and average density on the hierarchical system, k_h , the flow and
 26 density on each of the local and arterial roads can be obtained by solving the set of equations given
 27 by (1.2), (2) and the MFD relationships, $q_i = Q_i(k_i)$. The corresponding average flow in the
 28 system can then be obtained from (1.1). Thus, what is left to be determined is the value of p . The
 29 remainder of this section considers two scenarios: 1) vehicles route themselves to minimize their
 30 personal travel time (user equilibrium); and, 2) vehicles are routed to minimize the total travel time
 31 in the system (system optimum).

1

2 *User equilibrium (UE) conditions*

3 This section considers the case in which vehicles behave as according to Wardrop's first principle
 4 (41) and route themselves in such a way as to minimize their own personal travel time. Consider
 5 the average travel times using option 1, $tt_1(k_H, p)$, and option 2, $tt_2(k_H, p)$, as a function of total
 6 network density k_H and fraction of vehicles using strategy 1 p :

$$8 \quad tt_1(k_H, p) = \sum_z P_z \times \left(\frac{D_l^1(z)}{V_l(k_l)} + \frac{D_a^1(z)}{V_a(k_a)} \right) \\ 7 \quad = p_l^2 \times \frac{D}{V_l(k_l)} + 2 \times p_l p_a \times \left(\frac{D-S/2}{V_l(k_l)} + \frac{S/2}{V_a(k_a)} \right) + p_a^2 \times \left(\frac{D-S}{V_l(k_l)} + \frac{S}{V_a(k_a)} \right) \quad (3.1)$$

$$10 \quad tt_2(k_H, p) = \sum_z P_z \times \left(\frac{D_l^2(z)}{V_l(k_l)} + \frac{D_a^2(z)}{V_a(k_a)} \right) \\ 9 \quad = p_l^2 \times \left(\frac{S}{V_l(k_l)} + \frac{D-S}{V_a(k_a)} \right) + 2 \times p_l p_a \times \left(\frac{S/2}{V_l(k_l)} + \frac{D-S/2}{V_a(k_a)} \right) + p_a^2 \times \frac{D}{V_a(k_a)} \quad (3.2)$$

11 The optimal routing strategy under user equilibrium conditions for any k_h would be that
 12 which provides travel times such that no vehicles can reduce their travel times by changing routing
 13 options. This can be found from the following optimization problem:

$$14 \quad \min_p \int_0^p tt_1(k_H, p) dp + \int_0^{1-p} tt_2(k_H, p) dp \quad (4)$$

15 which is subject to (1.2), (2), the MFD relationships and non-negativity constraints. Note that these
 16 equations assume that p is the same for each OD pair. This can be easily relaxed in Equation (2);
 17 however, doing so does not significantly change the final MFD estimation while increasing the
 18 complexity of the formulation and analytical solution. Thus, this assumption is maintained for
 19 simplicity.

20

21 *System optimum (SO) conditions*

22 Under Wardrop's second principle, vehicles select between the competing options to minimize the
 23 average travel time of all vehicles, \bar{tt} , in the network. In this case, the solution is found using the
 24 following optimization problem:

$$25 \quad \min_p \bar{tt}(p) = \min_p p \times tt_1(p) + (1-p) \times tt_2(p) \quad (5)$$

26 This condition can be proven to be equivalent to the condition required to maximize the average
 27 flow (q_H) in the system for a given average system density.

28

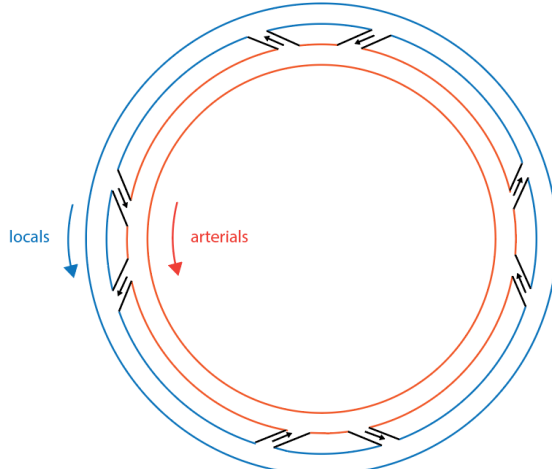
1 **Simulation verification**

2 A simulation of an infinite arterial corridor (i.e., ring road) is used to validate the MFDs obtained
 3 from the analytical derivations. This section describes the simulation parameters and compare the
 4 results with the analytical model.

5

6 *Simulation description*

7 In this section, a dual ring network is simulated to study the MFD of a hierarchical one-way
 8 corridor. The network simulated here—shown in FIGURE 2—consists of two one-way streets
 9 arrange to form concentric rings. One ring represents the arterial streets while the other the locals.
 10 The arterial street is assumed to have travel lane on which traffic obeys a triangular fundamental
 11 diagram with a free flow speed (40 mile/hour), capacity (2000 vehicle/hour) and jam density (250
 12 vehicle/mile). Each local street also has one travel lane on which traffic obeys a triangular
 13 fundamental diagram with a common free flow speed (20 mile/hour), capacity (1000 vehicle/hour)
 14 and jam density (250 vehicle/mile). Vehicles can only travel between the two roadway types at
 15 predesignated points located every 1 mile.



16
 17

FIGURE 2. Simulated hierarchical one-way linear corridor.

18 Vehicles on the network were simulated using the cellular automata model (CAM)
 19 proposed by Daganzo (42), which is consistent with kinematic wave theory (43–45). In this
 20 framework, each street is broken up into homogeneous discrete cells of length 0.004 miles (equal
 21 to average vehicle spacing at jam density), which allows only a single vehicle to occupy any cell
 22 at any time period. Vehicle locations on arterials are updated at consistent intervals of 0.36 seconds
 23 while vehicle locations on local roads are updated at consistent intervals of 0.72 seconds. Average
 24 flow and density across the entire network are computed using the generalized definitions proposed
 25 by Edie (39) at discrete intervals of 6 minutes.

26 The simulation starts with an empty network. Vehicles gradually enter the network with
 27 their origins and destinations uniformly distributed across all arterial and local streets until the
 28 average density of the network reaches a predefined value. This density is then maintained for the
 29 length of the simulation run. To do this, vehicles that arrive are to their destination are immediately

1 replaced by a randomly generated new trip. In the results shown here, the distance traveled for an
2 individual trip is drawn randomly from a uniform distribution between 8 miles to 12 miles.

3 Under user equilibrium assumption, each vehicle chooses its travel strategy based on the
4 estimated travel time calculated using the average speed of local roads and arterials of the last 1-
5 minute period by the time it enters the network. Under system optimal assumption, multiple
6 simulations are run with density of arterials kept around different pre-determined values by
7 controlling the number of vehicles that uses strategy 2. The simulation with pre-determined arterial
8 density that maximizes the average network flow is then used to obtain the MFD under system
9 optimal assumption.

10

11 *Comparison of analytical and simulation results*

12 In this section, some key features of MFDs for one-way hierarchical linear corridor under user
13 equilibrium assumption and system optimal assumption are identified by comparing analytical and
14 simulation results.

15

16 User equilibrium routing

17 **Error! Reference source not found.a** illustrates the fundamental diagrams for local and arterial
18 roads, as well as the analytically derived MFD for the corridor and observed flow-density
19 relationship in the simulation under user equilibrium routing conditions. As expected, the UE
20 MFDs fall somewhere between the individual fundamental diagrams of the local roads and
21 arterials. The network-wide flow-density relationships obtained analytically and from the
22 simulation are remarkably consistent, particularly in the uncongested and capacity regimes. Small
23 differences between the simulated and analytical MFDs occur when the network is highly
24 congested. This is likely due to the tendency of ring networks to become imbalanced and
25 gridlocked when heavily congested (14, 46).

26 Notice that the network-wide MFD is not unimodal or concave under user equilibrium
27 routing conditions. In **Error! Reference source not found.a**, flow increases with density in the
28 range $k_H \in (0, 28)$, decreases in the range $k_H \in (28, 44)$, increases again in the range $k_H \in (44, 67)$, and finally decreases from $k_H \in (67, 250)$. Examination of **Error! Reference source**
29 **not found.b**, which plots the density on each individual roadway type as a function of the average
30 density, reveals that the latter decreasing section represents the congested branch in which both
31 the local and arterial roads are congested, while the former decreasing section represents cases in
32 which the arterial is congested but local roads are not. This non-concave shape is particularly
33 interesting as most MFD-based modeling frameworks in the research literature rely on the
34 assumption of a unimodal, concave MFD. Repeated tests show that this non-unimodal and non-
35 concave shape is a general finding under various scenarios and settings in both the simulation
36 environment and analytical derivation in user equilibrium routing conditions.

37

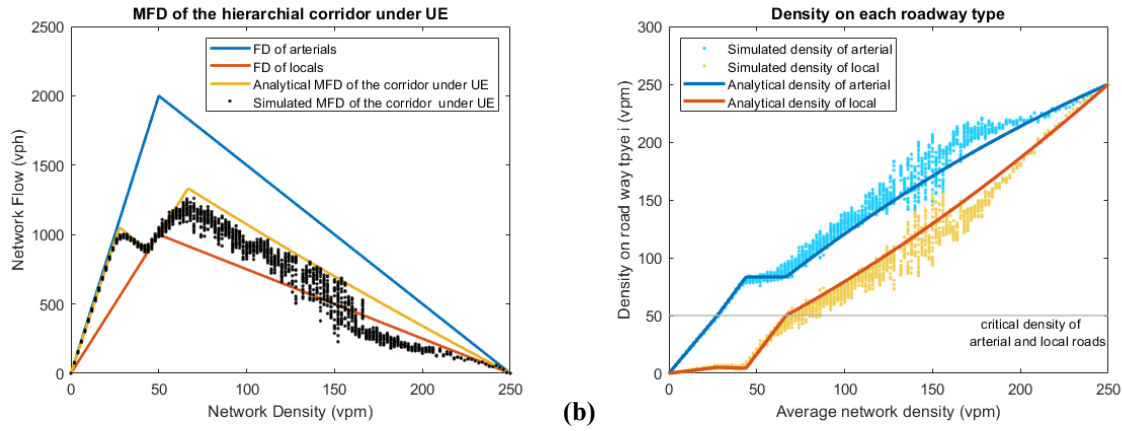


FIGURE 3. Comparison of (a) MFDs and (b) densities on individual roadway types for hierarchical corridor under user equilibrium conditions.

System optimal routing

Error! Reference source not found.a provides the fundamental diagrams for the local and arterial roads, as well as MFDs obtained analytically and from the simulation under system optimal routing conditions, while **Error! Reference source not found.**b provides the density on each individual roadway type as a function of the average network density for this case. Great consistency is observed between the analytically obtained and simulated flow-density relationship in the uncongested and near-capacity regimes. However, the simulation results show that the network becomes unstable when it starts to congested. Differences between the analytically derived MFD and the MFD observed in the simulations tend to grow as the network becomes more congested. Several reasons account for this discrepancy problem:

1) As in the UE case, the network has the tendency towards inhomogeneous congestion distributions and will produce non-MFD states as it gets congested and unstable, as identified in many previous works (14, 15, 17, 46).

2) Constraint (2) which provides the relationship between flow of the two roadway types is only valid in a long stable period where all vehicles should be able to finish their trips. However, in the simulations, when the network gets so congested that many vehicles cannot finish their trip in the simulated period, the flow relationship will not be the same as the analytical solution suggested.

3) Bottlenecks arise at the transition points between locals and arterials. The analytical solution suggests that the arterial should be always used with flow as high as possible, which makes the local roads have a high density and a low flow when the network is congested. The significant discrepancy between flow of the two roadway types makes it extremely difficult for vehicles to turn from arterials to the local roads in the linear corridor. As a result, bottlenecks may form at the transition points, which makes the network highly unstable.

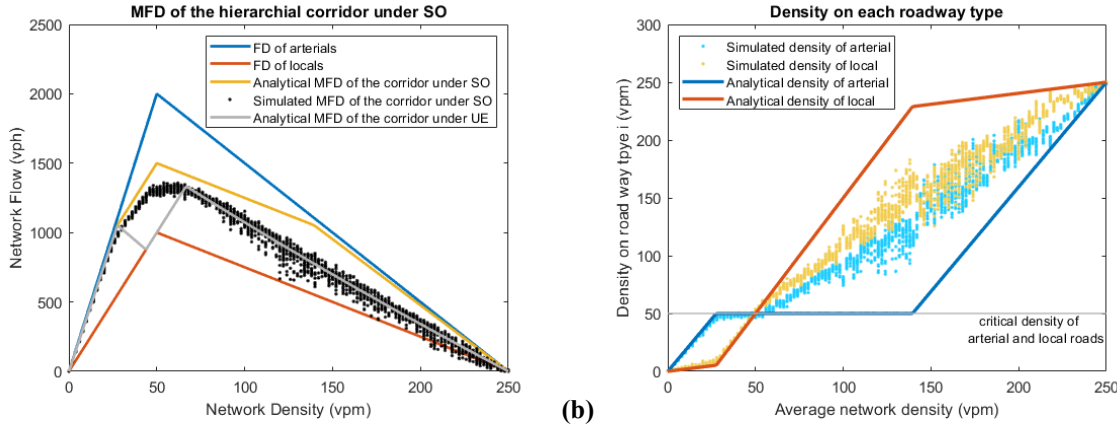


FIGURE 4. Comparison of (a) MFDs and (b) densities on individual roadway types for hierarchical corridor under system optimal conditions.

Differences between **Error! Reference source not found.** and **Error! Reference source not found.** indicate that vehicles tend to use arterials more than locals to minimize their own travel time under user equilibrium condition. By contrast, arterials are used at their capacity under the system optimal condition, which provides the higher overall flow and lowest travel time to all vehicles in the network. This suggests that hierarchical networks can be made more productive by carefully routing vehicles within the network. Comparison of the UE and SO MFDs also shows that the MFDs are unimodal and concave in the SO, whereas they are not in the UE case.

Applications for hierarchical street network design

For a hierarchical one-way linear corridor, two roadway features affect the network MFD: the spacing of the transition points where vehicles can switch roadway types and the MFD of each roadway type. This section demonstrates how the analytical model—which provides a reasonable estimate of the MFDs under both UE and SO conditions, except when the network is highly congested—can be used to understand the impact of these features on the network MFD. This information can be used to inform network design decisions related to these features.

Spacing of the transition points

The following numerical example illustrates how spacing of transition points can affect MFD of a one-way linear corridor. FIGURE 5a and FIGURE 5b illustrate the MFDs of the entire hierarchical system with different spacings under UE and SO routing assumptions, respectively, assuming the same FD for the local and arterial networks as in the previous section. Under UE routing conditions, smaller transition spacings lead to higher flows at low network densities. However, larger transition spacings have a higher first apex of the MFD. The rest of the MFD is insensitive to this spacing. Since maximizing network flow at or near these peaks is most critical to accommodate surges in demand, a larger transition spacing would be preferred under UE routing conditions. By contrast, smaller transition spacings lead to higher network flow for most part of the uncongested regime and congested regime under SO conditions.

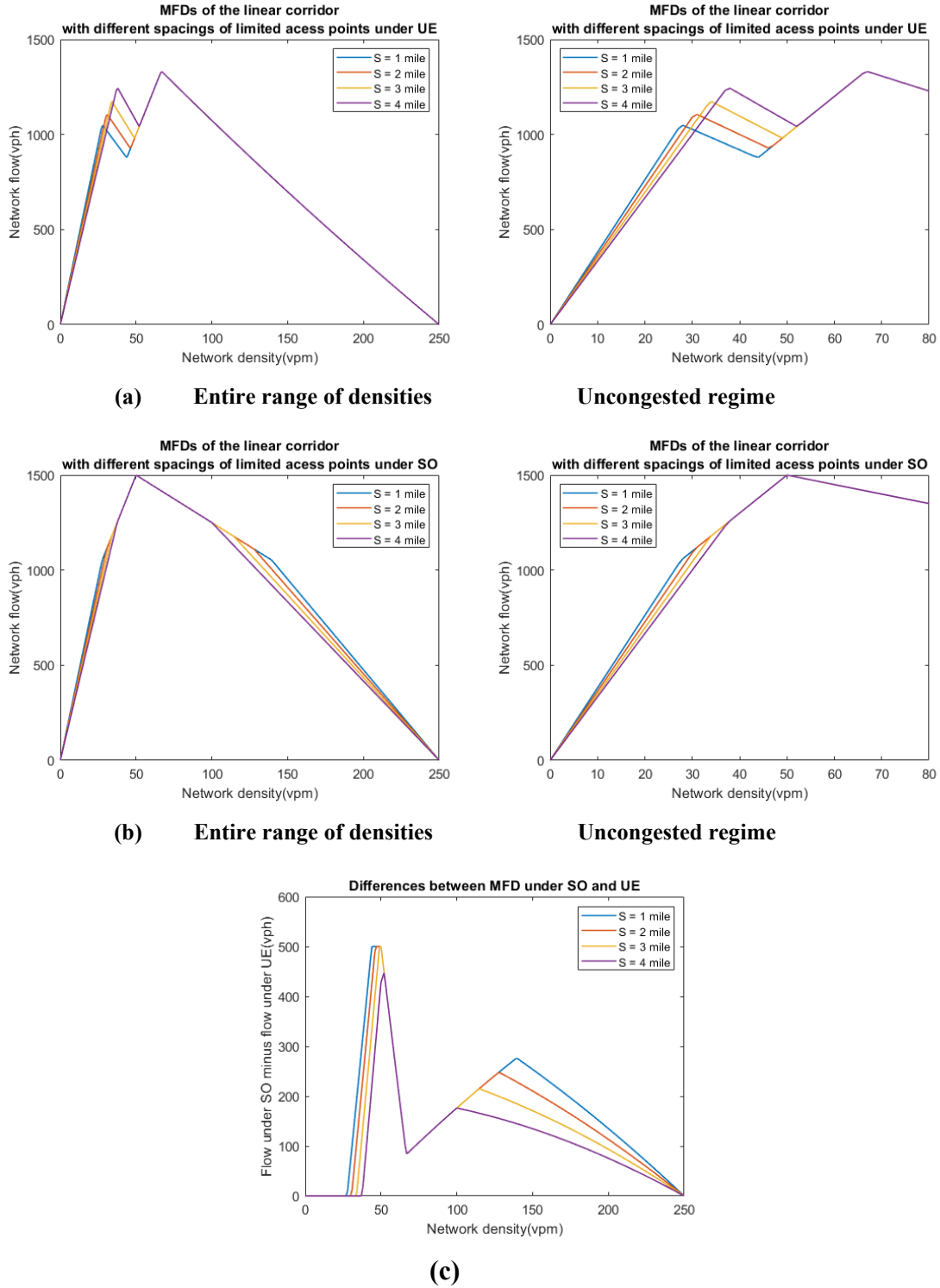


FIGURE 5. (a) Comparison of MFDs for linear corridors with different spacings of transition points under UE conditions; (b) Comparison of MFDs for linear corridors with different spacings of transition points under SO conditions; and, (c) Differences between MFD under SO condition and MFD under UE condition

1 FIGURE 5c shows the difference in average flows observed for each density under the SO
 2 and UE conditions. This is related to the price of anarchy or the loss in network efficiency that
 3 occurs by allowing travelers free will to make routing decisions. As expected, this difference is
 4 greater than or equal to zero for all spacing values, since the SO MFD is always greater than or
 5 equal to the UE MFD. In general, the difference between the SO and UE flows decreases with the
 6 transition spacing. This occurs because vehicles have to travel longer distances before switching
 7 between roadway types as the transition spacing increases, and this results in the decision variable
 8 p having a reduced impact on the network MFD. Therefore, even if different p values are obtained
 9 for the UE and SO cases, the resulting MFDs will be close.

10 By understanding how these two routing assumptions impacts the MFD, agencies can
 11 design the network based on their objectives and how much flexibility travelers have in routing. If
 12 agencies care about user equilibrium allowing people to choose their paths that minimize their own
 13 travel time, then a smaller spacing is preferred. If agencies seek to minimize the difference between
 14 observed network efficiency and maximum network efficiency (i.e., the price of anarchy) or have
 15 limited ability to induce certain routing behaviors, a larger spacing is preferred as it results in
 16 smaller difference between MFD of the two routing conditions.

17

18 *Signals at the transition points*

19 The presence of signals at the transition points between the arterials and local roads can
 20 dramatically impact both safety performance, as well as the fundamental diagrams of both the local
 21 and arterial roadways and the overall network MFD. Here, we assume two-phase signals are
 22 implemented at all transition points with one phase for all movements of arterials and the other for
 23 all movements of local roads. The impact of green time allocation between the arterials and the
 24 local roads on the overall network MFD is examined. Consider the following example with same
 25 arterial and local roads as before. Assume the spacing of the transition points is 1 mile and the
 26 cycle length of the signals at the transition points is 60 seconds. The MFDs of arterial and locals
 27 under different signal settings are obtained using the method of cuts (28), which accounts for green
 28 time allocation between the two street types.

29 FIGURE 6a illustrates how the UE MFD changes with the signal allocation at the transition
 30 points. It is worth noting that the functional form of the network MFD under UE condition becomes
 31 unimodal when the effects of signals are added but is still non-concave. For the free flow regime,
 32 the system-wide flow increases with the proportion of the cycle allocated to the arterial since
 33 arterials have a faster free flow speed than the local roads. The difference among MFDs under
 34 different signal allocations becomes even larger as soon as the first apex is reached. Moreover, a
 35 network with more green assigned to arterial has a higher capacity since the capacity of arterials
 36 becomes much higher than capacity of local roads. However, the network gets congested faster
 37 and has lower flow for the congested regime as more green time allocated to movements of
 38 arterials. Therefore, more green time should be allocated to arterials if the network is expected to
 39 operate at lower densities under UE conditions. On the contrary, cycle time should be more evenly
 40 allocated if the network is expected to operate at or near capacity since capacity flows can be
 41 maintained for a wider range of densities.

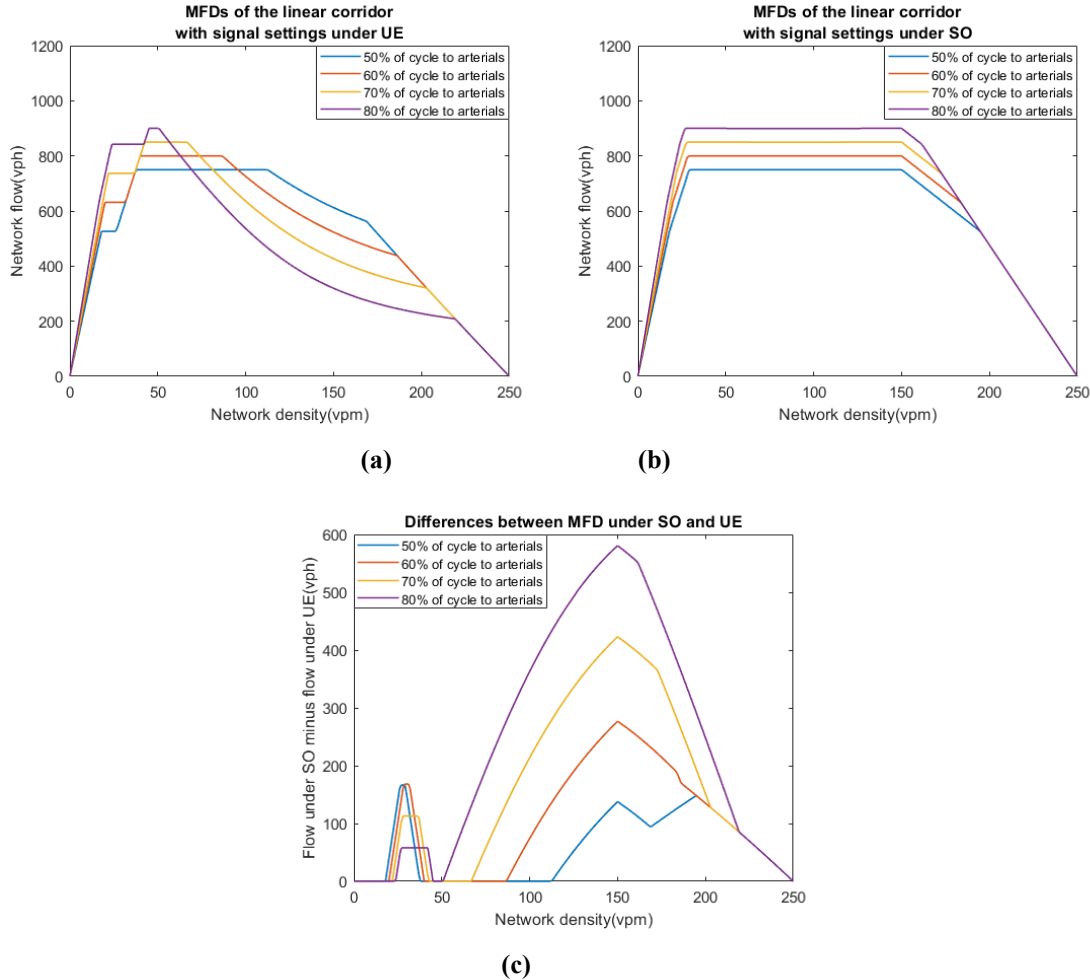


FIGURE 6. (a) Comparison of MFDs for linear corridors with different signal settings under UE; (b) Comparison of MFDs for linear corridors with different signal settings under SO; and, (c) Differences between MFD under SO condition and MFD under UE condition

FIGURE 6b shows the network MFD under SO conditions with different signals. It is clear that assigning more cycle time to arterials leads to higher flows for the entire range of network densities. Therefore, more green time should be assigned for the movements of arterials under SO conditions. FIGURE 6c provides the differences between network MFDs under system optimal and user equilibrium conditions. It is shown that signals with more green assigned to arterials results in smaller differences in flow in the free flow regime but more significant differences for the capacity and congested regimes. This indicate that while assigning more green time to arterials can improve network efficiency, it might lead to more reduced relative efficiency when users are allowed to route themselves.

1 HIERARCHICAL TWO-DIMENSIONAL NETWORK

2 Now, we extend the analytical formulations to obtain the MFD of a linear corridor to a two-
 3 dimensional network system with hierarchical roadways. Again, without loss of generality, we
 4 assume this system is composed of two street types that allow travel in two directions: arterials
 5 with N_a travel lanes in each direction, block length (l_a) and total length (L_a), and local roads with
 6 N_l travel lanes in each direction, block length (l_l) and total length (L_l). The arterials and locals are
 7 assumed to be arranged in a sequence such that there is one arterial for every $N \in \mathbb{Z} + \text{locals}$. An
 8 example for $N = 2$ is illustrated in FIGURE 7. One can easily prove the following two
 9 relationships:

10
$$l_a = (N + 1) \times l_l \quad (9.1)$$

11
$$r = \frac{L_l}{L_a} = \frac{N \times N_l}{N_a} \quad (9.2)$$

12 where r refers to the ratio of the total length of local roads to the total length of arterials.

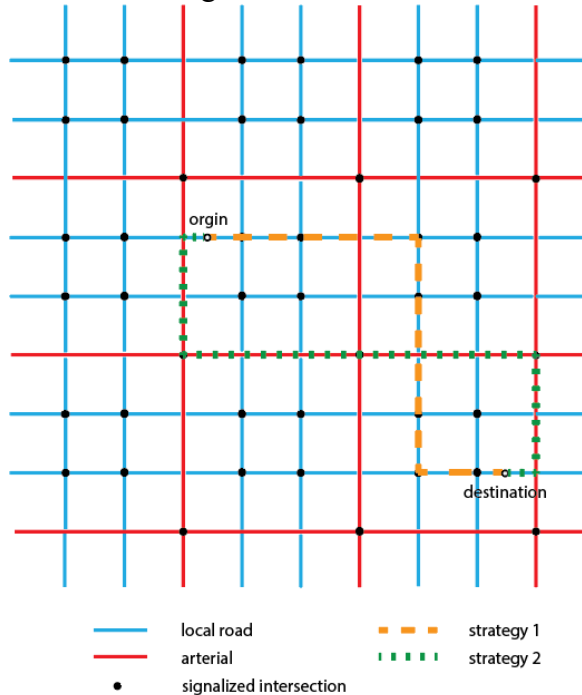


FIGURE 7. Two-dimensional hierarchical network

16 Again, vehicles cannot travel between the two roadway types freely. Instead, vehicles are
 17 only able to switch the two roadway types at the intersections of local roads and arterials.
 18 Intersections between arterials are assumed to be signalized, while intersections involving a local
 19 road are assumed to be stop-controlled. Moreover, we assume that all trips begin and end on the
 20 local roads.

21 The average flow (q_H) and density (k_H) of this system two-dimensional network can be
 22 determined using (1.1) and (1.2), respectively. As in the linear corridor, we assume that each

1 vehicle has two travel options: 1) mainly use local roads for their trip and only use arterials to
 2 access the nearest local road or approach their destination; or, 2) mainly use arterials for their trip
 3 and only use local roads to access the nearest arterial or approach their destination. The difference
 4 when these strategies are applied in the two-dimensional network is that a vehicle may experience
 5 additional total travel distance in order to access the nearest local road or arterial depending on its
 6 OD location. For example, FIGURE 7 shows the two travel strategies for one combination OD
 7 pair. We can see that when using strategy 1, local roads are used for the entire trip and thus there
 8 is no additional trip distance. When using strategy 2, in order to access the nearest arterial from
 9 the origin, the vehicle has additional travel distance to access the arterial streets.

10 TABLE 2 shows the percentage of each OD pair $P(z)$ and the average distance traveled
 11 per trip on roadway type i under each OD pair-routing option combination, $D_i^j(z)$, assuming ODs
 12 are uniformly distributed across the network.
 13

14 **TABLE 2. Average trip distance on each roadway type**

OD pair z	Percentage of OD pairs, $P(z)$	Strategy 1		Strategy 2	
		$D_l^1(z)$	$D_a^1(z)$	$D_l^2(z)$	$D_a^2(z)$
LL	$\frac{r^2}{(r+1)^2}$	D	0	$\frac{l_a}{3}$	$D - \frac{l_a}{48}$
LA	$\frac{r}{(r+1)^2}$	D	$\frac{l_l}{4}$	$\frac{l_a}{6}$	D
AL	$\frac{r}{(r+1)^2}$	D	$\frac{l_l}{4}$	$\frac{l_a}{6}$	D
AA	$\frac{1}{(r+1)^2}$	D	$\frac{l_l}{2}$	0	D

15
 16 Let p denote the fraction of vehicles that use routing strategy 1. The ratio of flow on the
 17 arterial and local roads would be related by the total distance traveled on each of the two roadway
 18 types can be defined similarly to (2) as follows:

$$19 \quad \frac{q_l}{q_a} = \frac{l_a}{l_l} \times \frac{p \times D + (1-p) \times \left[\frac{r^2}{(r+1)^2} \times \frac{l_a}{3} + \frac{2r}{(r+1)^2} \times \frac{l_a}{6} + \frac{1}{(r+1)^2} \times 0 \right]}{p \times \left[\frac{r^2}{(r+1)^2} \times 0 + \frac{2r}{(r+1)^2} \times \frac{l_l}{4} + \frac{1}{(r+1)^2} \times \frac{l_l}{2} \right] + (1-p) \times \left[\frac{r^2}{(r+1)^2} \times (D - \frac{l_a}{48}) + \frac{2r}{(r+1)^2} \times D + \frac{1}{(r+1)^2} \times D \right]} \quad (10)$$

20 The remainder of this section describes how MFD of the hierarchical two-dimensional
 21 network can be determined under user equilibrium and system optimum conditions.
 22

23 **Analytical method to obtain the system-wide MFD**

24 *User equilibrium (UE) conditions*

25 Under these assumptions, the corresponding average travel times of using option 1 and 2,
 26 respectively, are:

$$1 \quad tt_1(k_H, p) = \frac{r^2}{(r+1)^2} \times \frac{D}{V_l(k_l)} + \frac{2r}{(r+1)^2} \times \left(\frac{D}{V_l(k_l)} + \frac{\frac{l_l}{4}}{V_a(k_a)} \right) + \frac{1}{(r+1)^2} \times \left(\frac{D}{V_l(k_l)} + \frac{\frac{l_l}{2}}{V_a(k_a)} \right) \quad (11.1)$$

$$2 \quad tt_2(k_H, p) = \frac{r^2}{(r+1)^2} \times \left(\frac{\frac{l_a}{3}}{V_l(k_l)} + \frac{D - \frac{l_a}{48}}{V_a(k_a)} \right) + \frac{2r}{(r+1)^2} \times \left(\frac{\frac{l_a}{6}}{V_l(k_l)} + \frac{D}{V_a(k_a)} \right) + \frac{1}{(r+1)^2} \times \frac{D}{V_a(k_a)} \quad (11.2)$$

3 Under Wardrop's first principle, the optimal routing strategy for any k_h can be obtained
4 by solving (4), which subject to constraints (1.2), (9), (10) the MFD relationships and non-
5 negativity constraints. Again, the underlying assumption is that the value of p is the same for all
6 OD pair types. This assumption can be easily relaxed but does not change the final MFD
7 estimations in a significant way.

8

9 *System optimum (SO) conditions*

10 Under Wardrop's second principle of system optimality, the optimal routing strategy is found by
11 solving (5) which is subject to same constraints as the UE case.

12 Note that for a two-dimensional network, this condition is no longer necessarily equivalent
13 to the condition required to maximize the average flow (q_H) in the system for a given average
14 system density. This occurs because the average travel distance changes based on how vehicles
15 route themselves. However, if $D \gg l_l$ and $D \gg l_a$, the additional trip distance arising from
16 switching roadway type is negligible compared to D and the two conditions can be considered
17 equivalent.

18

19 **Numerical example**

20 In this section, some key features of MFDs for hierarchical two-dimensional networks are unveiled
21 using a numerical example. The local roads as assumed to have a block length of 300ft, a free flow
22 speed of 20 mph, capacity of 1000 veh/hr/lane and jam density of 250 veh/mi/lane. The arterial
23 roads have a free flow speed of 40 mi/hr, capacity of 2000 veh/hr/lane and jam density of 250
24 veh/mi/lane. Assume that all local roads have one travel lane in each direction while all arterials
25 have two travel lanes in each direction. The MFD of both local roads and arterial roads are obtained
26 using analytical methods based on variational theory (13) as a function of block length, signal
27 settings and fundamental diagram of individual links. Assume all signals have exactly the same
28 green period equal to half of the cycle length of 72 seconds. Moreover, vehicles are assumed to
29 travel an average distance of $D = 10$ mi.

30 FIGURE 8a and FIGURE 8b illustrates the MFDs for the local and arterial roads, as well
31 as the MFD of the entire hierarchical network under both the UE and SO optimal routing
32 assumptions. The MFDs are estimated for the cases when the number of local roads is 2 times and
33 5 times the number of arterials, respectively. From (9.1), we can obtain that the corresponding
34 block lengths of arterials are 900 ft ($N = 2$) and 1800 ft ($N = 5$), respectively.

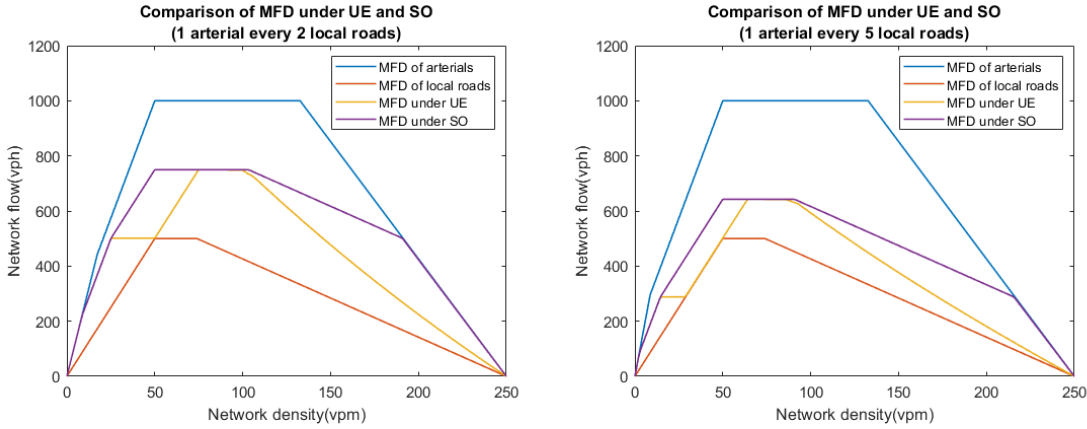


FIGURE 8. (a) Comparison of theoretical MFD for hierarchical network under UE and SO conditions when the number of local roads are 2 times the number of arterials; (b) Comparison of theoretical MFD for hierarchical network under UE and SO conditions when the number of local roads are 5 times the number of arterials

As expected, the network MFDs always fall somewhere between the individual MFDs of the local and arterial roadways and the MFD under SO routing always has higher flows for a given density than the MFD under UE routing conditions. Again, the MFD under UE routing condition is not concave, but is unimodal. By comparing FIGURE 8a and FIGURE 8b, it is clear that the ratio of the number of local roads to the number of arterials (N) not only has a great impact on the shape of MFD of arterials, but affects the shape and capacity of MFD of the hierarchical network as well. A smaller N indicates a denser arterial network, which leads to higher network flow and overall capacity under both UE and SO routing conditions. Note that if the arterial network is too dense (the block length of arterials is too short), the capacity of arterials will be significantly reduced due to queue spillovers.

Applications for hierarchical street network design

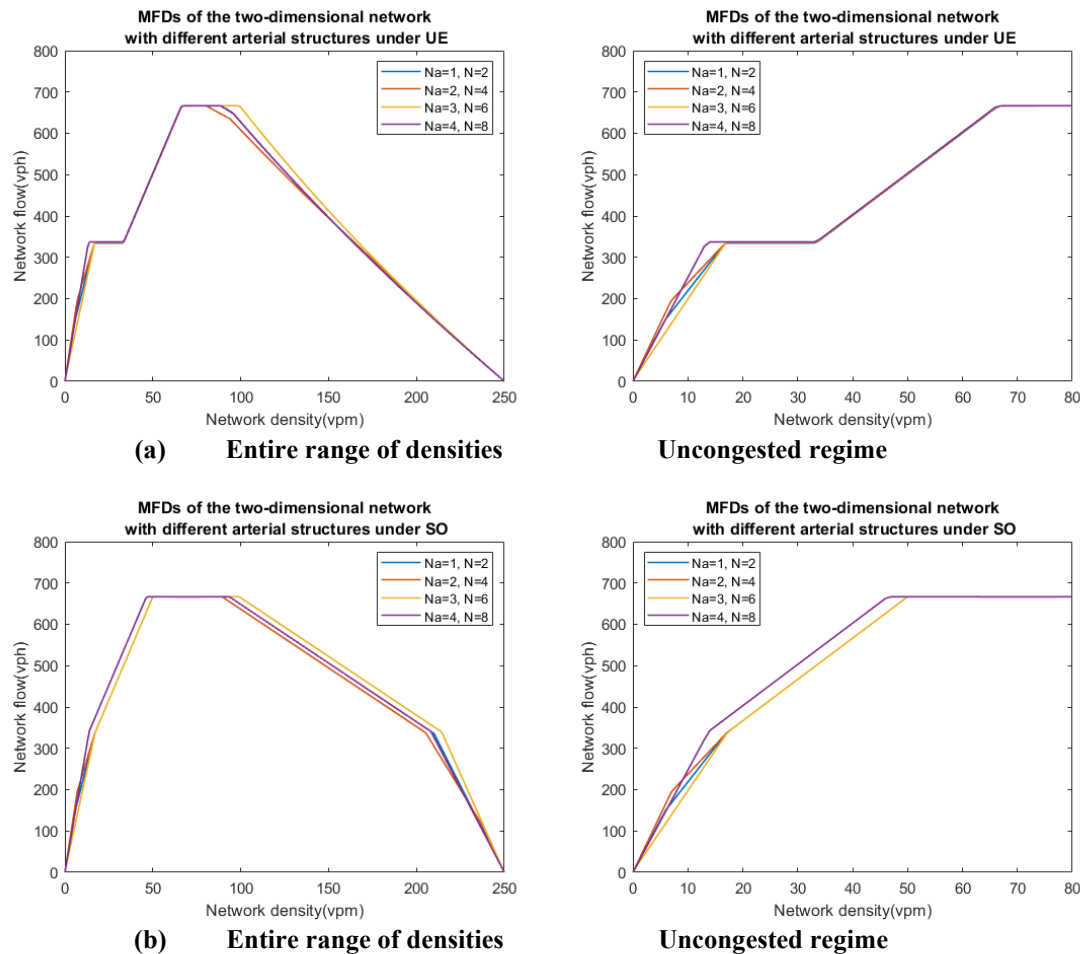
Consider the case where an arterial network will be created to supplement an existing local road grid network. This can be done by converting existing local roads to arterials by changing signal timings and potentially adding lanes. This presents a decision between selecting a choosing a sparser arterial network with more travel lanes or a denser arterial network with fewer travel lanes. Assume all local roads have one lane in each direction ($N_l = 1$). If the total lane-mile of the arterial network to construct is pre-determined, which means the ratio of total length of locals to total length of arterials r is fixed, then (8.2) yields:

$$r = \frac{L_l}{L_a} = \frac{N \times N_l}{N_a} = \frac{N}{N_a} \quad (14)$$

Consider the case in which that fundamental diagrams of local roads and arterials, block length of local roads, and signals settings are same as the numerical example in the previous section. Assume the average trip distance (D) is 5 miles. Block length of arterials are calculated from (8.1). The ratio of total length of local roads to total length of arterials r is assumed to be 2.

1 **Error! Reference source not found.a** and **Error! Reference source not found.b** shows
 2 how ratio of the number of local roads to the number of arterials roads (N) and the number of lanes
 3 each arterial has (N_a) jointly affect the network MFD. Overall, under both the UE and SO routing
 4 conditions, the arterial network with $N_a = 4$ and $N = 8$ contributes to a higher average network
 5 flow for the uncongested regime while the arterial network with $N_a = 3$ and $N = 6$ contributes to
 6 a higher average network flow for the congested regime. This indicates that for a fixed ratio of
 7 total length of locals to total length of arterials, there is a balance between the ratio of the number
 8 of local roads to the number of arterials roads and the number of arterial lanes that will maximize
 9 the average network flow for a given range of average network density.

10

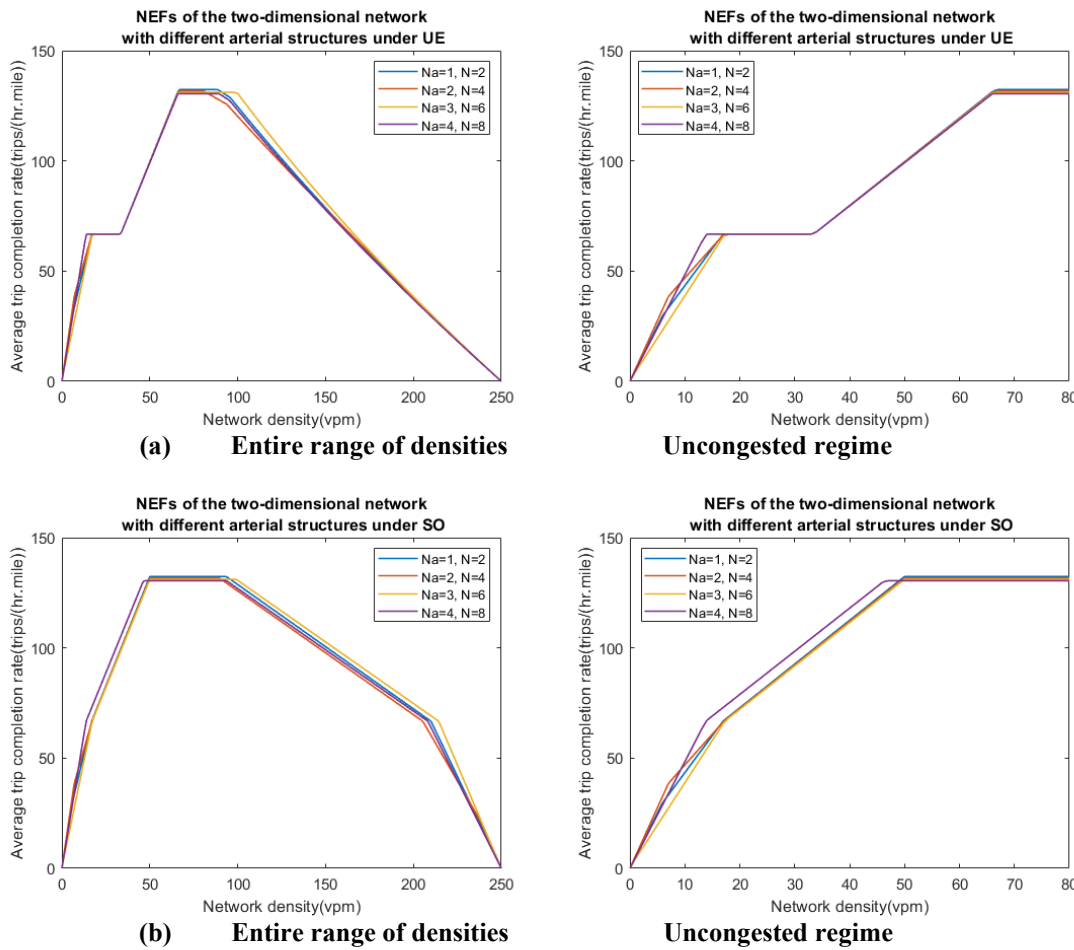


15 **FIGURE 9. (a) Comparison of MFDs for two-dimensional networks with different arterial structures under**
 16 **UE conditions; (b) Comparison of MFDs for two-dimensional networks with different arterial structures**
 17 **under SO conditions**

18 As is proven previously, the real average trip distance depends on p and is larger than D
 19 due to the additional arising from switching roadway type. Settings that allows for a higher flow
 20 is likely to result in longer real total trip distance and thus does not necessarily indicate a more
 21 efficient network. Therefore, instead of using network MFD, Gayah and Daganzo (47) suggests
 22 that the efficiency of these networks be measured by the rate at which trips can be served. **Error!**

Reference source not found.a and Error! Reference source not found.b provide NEFs with different ratios of the number of local roads to the number of arterials roads (N) and different numbers of lanes each arterial has (N_a). The shapes of the NEFs are quite similar to the shapes of MFDs except for the capacity regime. The arterial network with $N_a = 1$ and $N = 2$ provides a higher capacity for the average trip completion rate because the corresponding short arterial block length enables vehicles to switch easily between arterial and local roads without travelling too much additional amount of distance. However, such a network is low in efficiency for both free-flow and congested regime. By contrast, the arterial network with $N_a = 4$ and $N = 8$, though is highly efficient for the free-flow regime, provides lowest capacity as vehicles have to travel a large amount of additional distance switching between the two roadway types. The difference of capacities among different network structure can be even more significant when D is small. Therefore, the optimal arterial network structure depends on the average trip distance and the average network density regime that are designed for.

14



19 **FIGURE 10. (a) Comparison of NEFs for two-dimensional networks with different arterial structures under**
20 **UE conditions; (b) Comparison of NEFs for two-dimensional networks with different arterial structures**
21 **under SO conditions**

22

1 DISCUSSION

2 This paper develops an analytical method to estimate the MFDs of hierarchical street networks
3 that should be generally expected in real-world MFDs. This method directly builds on a recent
4 study that considers the MFDs of simple networks with route choice by considering features that
5 are specific to hierarchical network structures. Since the performance of hierarchical networks
6 depends on how users route themselves in the network, the analytical method considers both user
7 equilibrium and system optimal routing conditions. The method is applied to a linear corridor and
8 then extended to a more realistic two-dimensional grid network. The analytical results in the linear
9 case are compared to MFDs obtained from a cellular automata simulation. The results are found
10 to match up quite well for the entire range of densities in the UE routing case, and well for free-
11 flow and capacity states in the SO routing case. Thus, the simulation results validate the use of the
12 analytical method for MFD estimation.

13 The analytical results reveal interesting findings into the functional form of hierarchical
14 network MFDs. In both the corridor and grid network case, MFDs obtained under user equilibrium
15 routing conditions are found to not be unimodal or concave, even though the MFDs of individual
16 street types are unimodal and concave. The non-unimodal nature of the MFDs of hierarchical street
17 networks is important as the assumption of a concave, unimodal MFD is common in almost all
18 MFD modeling frameworks to date. This assumption is then leveraged for optimization purposes
19 and in proofs when developing network-wide traffic control strategies using the MFD. However,
20 the findings here are not necessarily surprising. Most MFDs obtained from empirical data have
21 relatively few data points available from congested states. This could lead to inaccurate
22 conclusions about the MFD shape and functional form, especially if multiple peaks exist as would
23 be expected from the findings here. Furthermore, there is empirical and simulation evidence to
24 support the finding of non-unimodal and/or non-concave MFDs in the research literature. Some
25 examples are provided in FIGURE 11. In the San Francisco, MFD, there is a small range of
26 densities (highlighted) where average flow appears flat as density increases, only to increase again.
27 In Chicago, the free-flow branch has several slopes that appear to create a non-concave shape. In
28 Zurich, the free-flow branch of several MFDs appear to have what might be similar non-concave
29 features. All are examples of larger networks in which street types are likely to represent different
30 hierarchical levels.

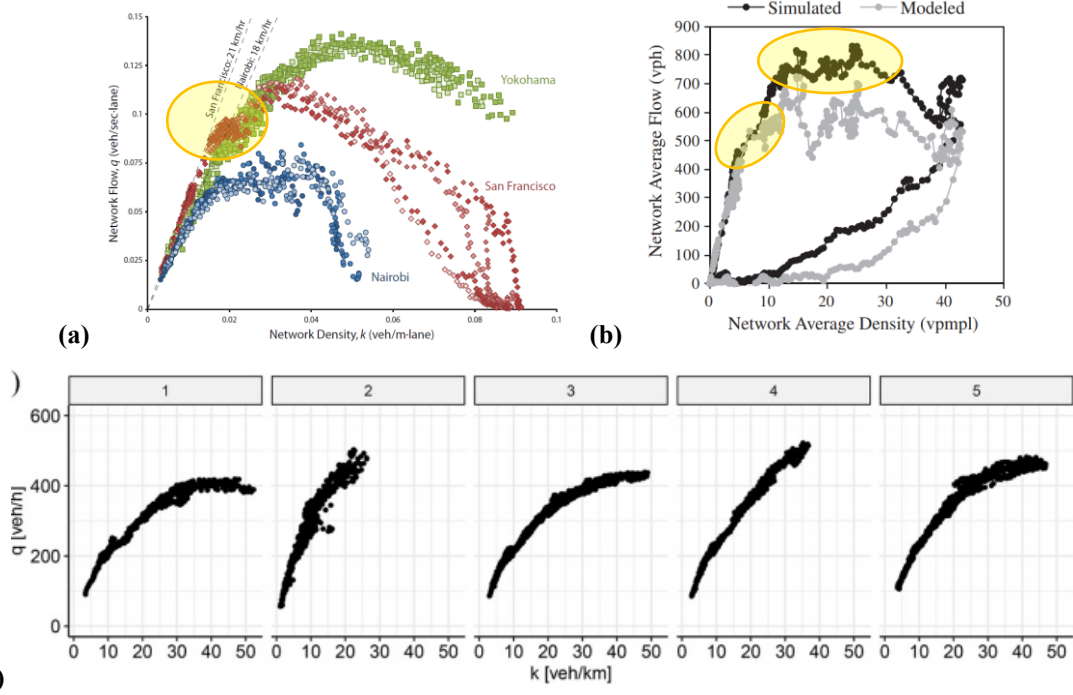


FIGURE 11. Example of potential non-concavity in functional form of MFDs in the literature. (a) San Francisco, California from simulation, taken from (48); (b) Chicago, Illinois from simulation, taken from (49); (c) Zurich, Switzerland from empirical data, taken from (27).

Applications of the proposed methodology to the design hierarchical street network structure are also discussed. For hierarchical one-way linear corridors, the numerical example indicates that the access to switch between the two roadway types should be constrained under UE routing conditions while easy access between the two roadway types should be provided under the SO routing conditions to achieve higher network flow. Moreover, application to signal design at the transition points is also provided. Under user equilibrium routing, more green time should be allocated to arterials when the network is expected to operate at low densities, while green time should be more evenly distributed if the network is expected to operate at capacity or in congestion. For hierarchical two-dimensional networks, a balance of number of arterial lanes and arterial density is shown to be important in designing the arterial network above an existing local road network.

Overall, this paper contributes to the growing literature on relationships between traffic variables aggregated across large spatial regions and how these relationships are influenced by network features. Future work should compare the MFDs of hierarchical two-dimensional network obtained from the proposed method with MFDs from simulation of network under more realistic conditions. Future work should also seek to develop analytical methods to account for bottlenecks at transition points between roadway types. Additional work is also needed to understand how route choice will affect turning movements at intersections, which should be considered in developing the functional form of the flow-density of a network.

AUTHOR CONTRIBUTION STATEMENT

The authors confirm contribution to the paper as follows: study conception and design: G. Xu, V. V. Gayah; analysis and interpretation of results: G. Xu, V. V. Gayah; draft manuscript preparation: G. Xu, V. V. Gayah. All authors reviewed the results and approved the final version of the manuscript.

REFERENCES

1. Godfrey, J. W. The Mechanism of a Road Network. *Traffic Engineering & Control*, Vol. 11, No. 7, 1969, pp. 323–327.
2. Mahmassani, H., J. C. Williams, and R. Herman. Investigation of Network-Level Traffic Flow Relationships: Some Simulation Results. *Transportation Research Record: Journal of the Transportation Research Board*, Vol. 971, 1984, pp. 121–130.
3. Mahmassani, H., J. C. Williams, and R. Herman. Performance of Urban Traffic Networks. 1987.
4. Geroliminis, N., and C. F. Daganzo. Existence of Urban-Scale Macroscopic Fundamental Diagrams: Some Experimental Findings. *Transportation Research Part B: Methodological*, Vol. 42, No. 9, 2008, pp. 759–770.
5. Daganzo, C. F. Urban Gridlock: Macroscopic Modeling and Mitigation Approaches. *Transportation Research Part B: Methodological*, Vol. 41, No. 1, 2007, pp. 49–62.
6. Haddad, J. Optimal Perimeter Control Synthesis for Two Urban Regions with Aggregate Boundary Queue Dynamics. *Transportation Research Part B: Methodological*, Vol. 96, 2017, pp. 1–25. <https://doi.org/10.1016/j.trb.2016.10.016>.
7. Ren, Y., Z. Hou, I. I. Sirmatel, and N. Geroliminis. Data Driven Model Free Adaptive Iterative Learning Perimeter Control for Large-Scale Urban Road Networks. *Transportation Research Part C: Emerging Technologies*, Vol. 115, 2020, p. 102618. <https://doi.org/10.1016/j.trc.2020.102618>.
8. Haitao, H., K. Yang, H. Liang, M. Menendez, and S. I. Guler. Providing Public Transport Priority in the Perimeter of Urban Networks: A Bimodal Strategy. *Transportation Research Part C: Emerging Technologies*, Vol. 107, 2019, pp. 171–192. <https://doi.org/10.1016/j.trc.2019.08.004>.
9. Gu, Z., S. Shafiei, Z. Liu, and M. Saberi. Optimal Distance- and Time-Dependent Area-Based Pricing with the Network Fundamental Diagram. *Transportation Research Part C: Emerging Technologies*, Vol. 95, 2018, pp. 1–28. <https://doi.org/10.1016/j.trc.2018.07.004>.
10. Yang, K., M. Menendez, and N. Zheng. Heterogeneity Aware Urban Traffic Control in a Connected Vehicle Environment: A Joint Framework for Congestion Pricing and Perimeter Control. *Transportation Research Part C: Emerging Technologies*, Vol. 105, 2019, pp. 439–455. <https://doi.org/10.1016/j.trc.2019.06.007>.
11. DePrator, A., O. Hitchcock, and V. V. Gayah. Improving Urban Street Network Efficiency by Prohibiting Left Turns at Signalized Intersections. *Transportation Research Record: Journal of the Transportation Research Board*, Vol. 2622, No. 1, 2017, pp. 58–69.

1 12. Ortigosa, J., V. V. Gayah, and M. Menendez. Analysis of One-Way and Two-Way Street
2 Configurations on Urban Grids. *Transportmetrica B: Transport Dynamics*, Vol. 7, No. 1,
3 2019, pp. 61–81.

4 13. Geroliminis, N., and J. Sun. Properties of a Well-Defined Macroscopic Fundamental
5 Diagram for Urban Systems. *Transportation Research Part B*, Vol. 45, No. 3, 2011, pp.
6 605–617. <https://doi.org/10.1016/j.trb.2010.11.004>.

7 14. Daganzo, C. F., V. V. Gayah, and E. J. Gonzales. Macroscopic Relations of Urban Traffic
8 Variables: Bifurcations, Multivaluedness and Instability. *Transportation Research Part B:
9 Methodological*, Vol. 45, No. 1, 2011, pp. 278–288.

10 15. Mazloumian, A., N. Geroliminis, and D. Helbing. The Spatial Variability of Vehicle
11 Densities as Determinant of Urban Network Capacity. *Philosophical Transactions of the
12 Royal Society A: Mathematical, Physical and Engineering Sciences*, Vol. 368, No. 1928,
13 2010, pp. 4627–4647.

14 16. Knoop, V., and S. Hoogendoorn. Empirics of a Generalized Macroscopic Fundamental
15 Diagram for Urban Freeways. *Transportation Research Record: Journal of the
16 Transportation Research Board*, Vol. 2391, 2013, pp. 133–141.
17 <https://doi.org/10.3141/2391-13>.

18 17. Saberi, M., A. Zockaie, and H. Mahmassani. Network Capacity, Traffic Instability, and
19 Adaptive Driving: Findings from Simulated Network Experiments. *EURO Journal on
20 Transportation and Logistics*, Vol. 3, No. 3–4, 2014, pp. 289–308.

21 18. Nagle, A. S., and V. V. Gayah. Accuracy of Networkwide Traffic States Estimated from
22 Mobile Probe Data. *Transportation Research Record: Journal of the Transportation
23 Research Board*, No. 2421, 2014, pp. 1–11. <https://doi.org/10.3141/2421-01>.

24 19. Leclercq, L., N. Chiabaut, and B. Trinquier. Macroscopic Fundamental Diagrams: A Cross-
25 Comparison of Estimation Methods. *Transportation Research Part B: Methodological*, Vol.
26 62, 2014, pp. 1–12.

27 20. Du, J., H. Rakha, and V. V. Gayah. Deriving Macroscopic Fundamental Diagrams from
28 Probe Data: Issues and Proposed Solutions. *Transportation Research Part C: Emerging
29 Technologies*, Vol. 66, 2016, pp. 136–149.

30 21. Ambühl, L., and M. Menendez. Data Fusion Algorithm for Macroscopic Fundamental
31 Diagram Estimation. *Transportation Research Part C: Emerging Technologies*, Vol. 71,
32 2016, pp. 184–197. <https://doi.org/10.1016/j.trc.2016.07.013>.

33 22. Buisson, C., and C. Ladier. Exploring the Impact of Homogeneity of Traffic Measurements
34 on the Existence of Macroscopic Fundamental Diagrams. *Transportation Research Record:
35 Journal of the Transportation Research Board*, No. 2124, 2009, pp. 127–136.

36 23. Tsubota, T., A. Bhaskar, and E. Chung. Brisbane Macroscopic Fundamental Diagram:
37 Empirical Findings on Network Partitioning and Incident Detection. *Transportation
38 Research Record: Journal of the Transportation Research Board*, No. 2421, 2014, pp. 12–
39 21.

40 24. Paipuri, M., Y. Xu, M. C. González, and L. Leclercq. Estimating MFDs, Trip Lengths and
41 Path Flow Distributions in a Multi-Region Setting Using Mobile Phone Data.

1 *Transportation Research Part C: Emerging Technologies*, Vol. 118, 2020, p. 102709.
2 <https://doi.org/10.1016/j.trc.2020.102709>.

3 25. Knoop, V. L., P. B. C. Van Erp, L. Leclercq, and S. P. Hoogendoorn. Empirical MFDs
4 Using Google Traffic Data. No. 2018-November, 2018, pp. 3832–3839.

5 26. Loder, A., L. Ambühl, M. Menendez, and K. W. Axhausen. Empirics of Multi-Modal
6 Traffic Networks – Using the 3D Macroscopic Fundamental Diagram. *Transportation
7 Research Part C: Emerging Technologies*, Vol. 82, 2017, pp. 88–101.
8 <https://doi.org/10.1016/J.TRC.2017.06.009>.

9 27. Ambühl, L., A. Loder, N. Zheng, K. W. Axhausen, and M. Menendez. Approximative
10 Network Partitioning for MFDs from Stationary Sensor Data. *Transportation Research
11 Record: Journal of the Transportation Research Board*, Vol. 2673, No. 6, 2019, pp. 94–
12 103. <https://doi.org/10.1177/0361198119843264>.

13 28. Daganzo, C. F., and N. Geroliminis. An Analytical Approximation for the Macroscopic
14 Fundamental Diagram of Urban Traffic. *Transportation Research Part B: Methodological*,
15 Vol. 42, No. 9, 2008, pp. 771–781.

16 29. Laval, J. A., and F. Castrillón. Stochastic Approximations for the Macroscopic Fundamental
17 Diagram of Urban Networks. *Transportation Research Part B*, Vol. 81, 2015, pp. 904–916.

18 30. Leclercq, L., and N. Geroliminis. Estimating MFDs in Simple Networks with Route Choice.
19 *Transportation Research Part B: Methodological*, Vol. 57, 2013, pp. 468–484.

20 31. Dakic, I., L. Ambühl, O. Schümperlin, and M. Menendez. On the Modeling of Passenger
21 Mobility for Stochastic Bi-Modal Urban Corridors. *Transportation Research Part C:
22 Emerging Technologies*, 2019. <https://doi.org/10.1016/j.trc.2019.05.018>.

23 32. Xu, G., Z. Yu, and V. V. Gayah. Analytical Method to Approximate the Impact of Turning
24 on the Macroscopic Fundamental Diagram. *Transportation Research Record: Journal of
25 the Transportation Research Board*, 2020, p. 036119812093327. <https://doi.org/10.1177/0361198120933274>.

27 33. Daganzo, C. F. A Variational Formulation of Kinematic Waves: Basic Theory and Complex
28 Boundary Conditions. *Transportation Research Part B: Methodological*, Vol. 39, No. 2,
29 2005, pp. 187–196.

30 34. Daganzo, C. F., and M. Menendez. A Variational Formulation of Kinematic Waves:
31 Bottleneck Properties and Examples. 2005.

32 35. Daganzo, C. F., and L. J. Lehe. Traffic Flow on Signalized Streets. *Transportation Research
33 Part B: Methodological*, Vol. 90, 2016. <https://doi.org/10.1016/j.trb.2016.03.010>.

34 36. Ortigosa, J., and M. Menendez. Traffic Performance on Quasi-Grid Urban Structures.
35 *Cities*, Vol. 36, 2014, pp. 18–27.

36 37. Knoop, V. L., D. De Jong, and S. Hoogendoorn. The Influence of the Road Layout on the
37 Network Fundamental Diagram. 2014.

38 38. Muhlich, N., V. V. Gayah, and M. Menendez. An Examination of MFD Hysteresis Patterns
39 for Hierarchical Urban Street Networks Using Micro-Simulation. *Transportation Research
40 Record: Journal of the Transportation Research Board*, No. 2491, 2015, pp. 117–126.

1 39. Edie, L. C. Discussion of Traffic Stream Measurements and Definitions. 1965.

2 40. Daganzo, C. F. *Public Transportation Systems: Basic Principles of System Design, Operations Planning and Real-Time Control*. Institute of Transportation Studies, University of California, Berkeley, 2010.

3 41. Wardrop, J. G. Some Theoretical Aspects of Road Traffic Research. No. 1, 1952, pp. 325–362.

4 42. Daganzo, C. F. In Traffic Flow, Cellular Automata = Kinematic Waves. *Transportation Research Part B: Methodological*, Vol. 40, No. 5, 2006, pp. 396–403.

5 43. Lighthill, M. J., and G. B. Whitham. On Kinematic Waves. I. Flood Movement in Long Rivers. *Proceedings of the Royal Society of London. Series A. Mathematical and Physical Sciences*, Vol. 229, No. 1178, 1955, pp. 281–316.

6 44. Lighthill, M. J., and G. B. Whitham. On Kinematic Waves. II. A Theory of Traffic Flow on Long Crowded Roads. *Proceedings of the Royal Society of London. Series A. Mathematical and Physical Sciences*, Vol. 229, No. 1178, 1955, pp. 317–345.

7 45. Richards, P. I. Shock Waves on the Highway. *Operations Research*, Vol. 4, No. 1, 1956, pp. 42–51.

8 46. Gayah, V. V., X. (Shirley) Gao, and A. S. Nagle. On the Impacts of Locally Adaptive Signal Control on Urban Network Stability and the Macroscopic Fundamental Diagram. *Transportation Research Part B: Methodological*, Vol. 70, 2014, pp. 255–268. <https://doi.org/10.1016/j.trb.2014.09.010>.

9 47. Gayah, V. V., and C. F. Daganzo. Analytical Capacity Comparison of One-Way and Two-Way Signalized Street Networks. *Transportation Research Record: Journal of the Transportation Research Board*, No. 2301, 2012, pp. 76–85.

10 48. Gonzales, E. J., C. Chavis, Y. Li, and C. F. Daganzo. Multimodal Transport in Nairobi, Kenya: Insights and Recommendations with a Macroscopic Evidence-Based Model. 2011.

11 49. Mahmassani, H. S., M. Saberi, and A. Zockaie. Urban Network Gridlock: Theory, Characteristics, and Dynamics. *Transportation Research Part C: Emerging Technologies*, Vol. 36, 2013, pp. 480–497.

12 29